Matrix Photochemistry of the Chlorocarbonyl Sulfenyl Compounds ClC(O)SY, with Y = Cl or CH_3

Rosana M. Romano,*,† Carlos O. Della Védova,†,‡ and Anthony J. Downs§

CEQUINOR (CONICET) and Laboratorio de Servicios a la Industria y al Sistema Científico (UNLP-CIC-CONICET), Departamento de Química, Facultad de Ciencias Exactas, Universidad Nacional de La Plata, 47 esq. 115, (1900) La Plata, Argentina, and Inorganic Chemistry Laboratory, University of Oxford, South Parks Road, Oxford, OX1 3QR, U.K.

Received: March 19, 2004; In Final Form: June 7, 2004

The photochemistries of the molecules ClC(O)SCl and $ClC(O)SCH_3$ (in both their normal and perdeuterated forms) isolated in solid Ar or N_2 matrixes at 15 K have been investigated. On the basis of evidence of the IR spectra of the matrixes, the products of irradiation with broad-band UV−visible light ($200 \leq \lambda \leq 800$ nm) were identified, thereby revealing quite different photochemical behaviors for the two molecules. ClC(O)SCl is subject to multichannel changes that include interconversion of the syn and anti rotamers, photodecomposition to give CO and SCl_2, formation of the hitherto unknown radical $ClC(O)S^{\bullet}$, and subsequent decomposition of this radical to give either the $ClCO^{\bullet}$ radical or the OCS molecule. By contrast, $ClC(O)SCH_3$ decomposes in two steps, the first consisting of fragmentation to CO and $ClSCH_3$, and the second entailing detachment of a hydrogen atom from the methyl group of $ClSCH_3$ with the formation of the molecular complex $H_2C{=}S\cdots HCl$. The IR spectra of both the $ClC(O)S^{\bullet}$ radical and $H_2C{=}S\cdots HCl$ have been interpreted with reference to the spectra predicted by ab initio and density functional theory methods.

Introduction

The La Plata research group has been interested in recent years in the structural, and particularly the conformational, properties of carbonyl sulfenyl derivatives of the type XC(O)SY and in gaining a detailed understanding of the photochemical behaviors of these compounds when isolated in solid inert matrixes at cryogenic temperatures. Three aspects of the rich matrix photochemistry that has thus come to light are noteworthy:

(i) The studies reveal photochemical interconversion between the more stable syn conformer and the anti conformer. This has been observed for several members of the sulfenyl carbonyl family, for example, FC(O)SCl,[1] FC(O)SBr,[2] FC(O)SNSO,[3] FC(O)SSC(O)F,[4] ClC(O)SBr,[5] $CH_3C(O)SH$,[6] and $FC(O)SCH_3$.[7]

(ii) The isolation, identification, and characterization of a variety of novel molecules have been achieved through photodecomposition of sulfenyl carbonyl compounds, including for example, sulfur (II) halides, such as BrSF[2] and BrSCl,[5] as well as isomers of the parent molecules, for example, BrC(O)SCl (from ClC(O)SBr)[5] and ClC(O)SF (from FC(O)SCl).[8]

(iii) Interpretation of the photochemistry, made possible by identification of all the photoproducts and detailed studies of their behavior as a function of irradiation time, has led to the development of new routes for the preparation of novel compounds by photochemical reactions brought about in matrix conditions. The first reported example was the isolation of BrC(O)SBr[9] by photolysis of a mixture of Br_2 and OCS in an Ar matrix, a method suggested by detailed analysis of the matrix photochemistry of ClC(O)SBr.[5]

SCHEME 1: Photochemical Interconversion between the Syn and Anti Forms of XC(O)SY Compounds in Matrix Conditions.

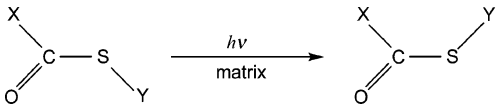

(1)

It is in this general context and as a second stage of our studies of the structural and vibrational properties of (chlorocarbonyl)-sulfenyl chloride, ClC(O)SCl, and methyl thiochloroformate, $ClC(O)SCH_3$,[10] that we report here on the matrix photochemistry of these two molecules. To assist with the identification of the products formed on photolysis of $ClC(O)SCH_3$, we have also studied the matrix photochemistry of the perdeuterated compound. In addition, attribution to new species of some of the IR bands appearing on photolysis has been supported by ab initio and density functional theory (DFT) calculations.

Experimental and Computational Procedures

Experimental Methods. ClC(O)SCl and $ClC(O)SCH_3$ were purchased from Aldrich and subsequently purified by repeated trap-to-trap distillation in vacuo. $ClC(O)SCD_3$ was prepared for the first time by the reaction of $ClC(O)OCCl_3$ with CD_3SH (both ex-Aldrich) at ambient temperature, and subsequently purified by repeated trap-to-trap distillation. The matrix gases Ar and N_2 were used as supplied (both BOC, research grade).

Gas mixtures of ClC(O)SCl, $ClC(O)SCH_3$, or $ClC(O)SCD_3$, each taken severally with Ar or N_2 in the proportions ~1:1000, were prepared by standard manometric methods. Such a mixture

† CEQUINOR, Universidad Nacional de La Plata.
‡ Laboratorio de Servicios a la Industria y al Sistema Científico, Universidad Nacional de La Plata.
§ University of Oxford.

10.1021/jp048756y CCC: $27.50
Published on Web 08/03/2004

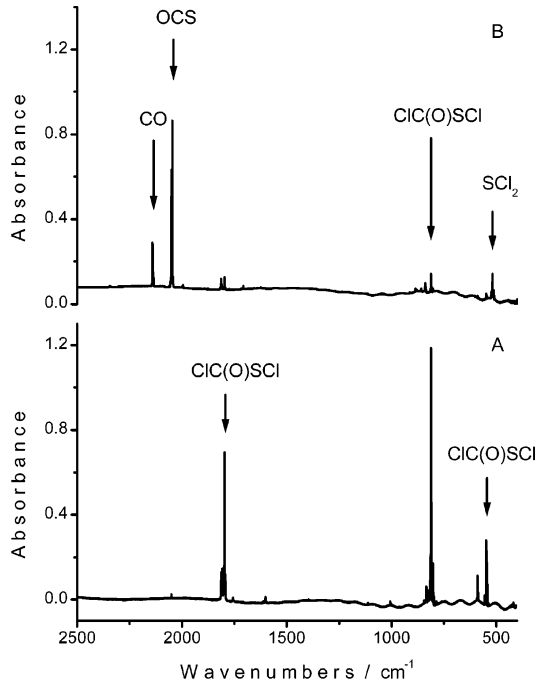

Figure 1. IR spectra of an Ar matrix containing ClC(O)SCl (A) following deposition and (B) after 120 min of broad-band UV−visible photolysis.

was then deposited on a CsI window cooled to ∼15 K by means of a Displex closed-cycle refrigerator (Air Products, model CS202) using the pulsed deposition technique.[11,12] IR spectra of the matrix samples were recorded at a resolution of 0.5 cm^{-1}, with 256 scans and an accuracy of ±0.1 cm^{-1}, using a Nicolet Magna-IR 560 FTIR instrument equipped with either an MCTB or a DTGS detector (for the range 4000−400 or 600−250 cm^{-1}, respectively). Following deposition and IR analysis of the resulting matrix, the sample was exposed to broad-band UV−visible radiation ($200 \leq \lambda \leq 800$ nm) from a Spectral Energy Hg−Xe arc lamp operating at 800 W. The output from the lamp was limited by a water filter to absorb IR radiation and so minimize any heating effects. The IR spectrum of the matrix was then recorded at different times of irradiation in order to monitor closely the decay and growth of the various absorptions. Experiments were also performed with a filter cutting out visible light and so confining the photolyzing radiation to wavelengths in the range 200−400 nm.

Computational Details. MP2 and DFT (B3LYP) calculations with a 6-31+G* basis set were performed using the Gaussian 98 program package[13] under the Linda parallel execution environment using two coupled personal computers.

Results and Discussion

Photolysis of ClC(O)SCl. Exposure of an Ar or N_2 matrix doped with roughly 0.1% ClC(O)SCl to broad-band UV−visible light ($200 \leq \lambda \leq 800$ nm) resulted in the decay of the bands due to ClC(O)SCl (as its syn conformer)[10] and the appearance and growth of new bands belonging to several different products. Attempts to achieve some photoselectivity were unavailing. Thus, UV light restricted to the range $\lambda = 200-400$ nm had the same effect as broad-band UV−visible light, but the reduced flux of photoactive radiation in the filtered beam meant that the rate of change was appreciably slower. Figure 1 illustrates the difference between the IR spectrum of an Ar matrix after broad-band irradiation for 2 h and the spectrum recorded immediately after deposition, revealing the absorptions that develop as a result of the photolysis. As reported previously,[10] some of the new bands can be assigned to the less stable anti conformer of ClC(O)SCl. These absorptions, which occur at 1701 and 870 cm^{-1} for an Ar matrix, are already present as extremely weak features in the original spectrum, with intensities suggesting that the anti form makes up <1% of the vapor molecules at ambient temperatures.[10]

TABLE 1: Wavenumbers and Assignments of the IR Absorptions Appearing after Broad-Band UV−Visible Photolysis of ClC(O)SCl Isolated in an Ar or N_2 Matrix

		assignment		wavenumber
Ar matrix ν (cm^{-1})	N_2 matrix ν (cm^{-1})	molecule	vibrational mode	reported previously
2140.4	2145.7 2144.6	OC···Cl_2	νC=O	2140.7[a]
2137.9 2137.2	2139.6 2137.2	CO	νC=O	2138.2[a]
2050.7 2049.6 2046.9 2043.1	2057.9 2056.0 2054.2 2053.5 2052.4	OCS	νC=O	2049.3[b]
1998.0 1994.3	2005.2 2003.1 2000.9 1999.5	O^{13}CS	νC=O	2000[b]
1892.5 1888.8 1876.7	1896.3 1894.0	ClCO•	νC=O	1876.7[c]
1774.8 1773.7	1762.6 1760.4	ClCOS•	νC=O	
1714.3 1707.1	1712.7 1711.3	*anti*-ClC(O)SCl	νC=O	
1046.8 1045.2	1046.5 1044.1	OCS	2 δ(OCS)	1045[b]
913.5 908.9	919.9 918.5 917.8 915.6 914.1	ClCOS•		
886.5 885.4 883.9 881.9 879.3	895.4 894.7 892.7 888.9 886.7 884.8	*anti*-ClC(O)SCl	ν_{as}Cl−C−S	
859.5 857.3 839.5	848.8 843.7 835.0	OCS	νC=S	858[b]
520.2	526.5 524.5	SCl_2	$\nu_s{}^{35}Cl S^{35}Cl$	524.2[d]
517.5	521.6 520.9	SCl_2	$\nu_{as}{}^{35}Cl S^{35}Cl$	520.2[d]
515.2	519.5 518.5	SCl_2	$\nu_s{}^{35}Cl S^{37}Cl$	
512.8	515.6 514.6	SCl_2	$\nu_{as}{}^{35}Cl S^{37}Cl$	

[a] Ref 18. [b] Ref 14. [c] Ref 17. [d] Ref 16.

Table 1 lists the wavenumbers of all the IR absorptions that develop on photolysis. To distinguish the bands corresponding to the different species and help determine the sequence of the changes, the integrated intensities of the new bands have been plotted as a function of irradiation time, as depicted in Figure 2 for an Ar matrix. One family of absorptions of which the most intense occurs near 2050 cm^{-1} and is accompanied by much weaker features near 1046 and 859 cm^{-1} grows continu-

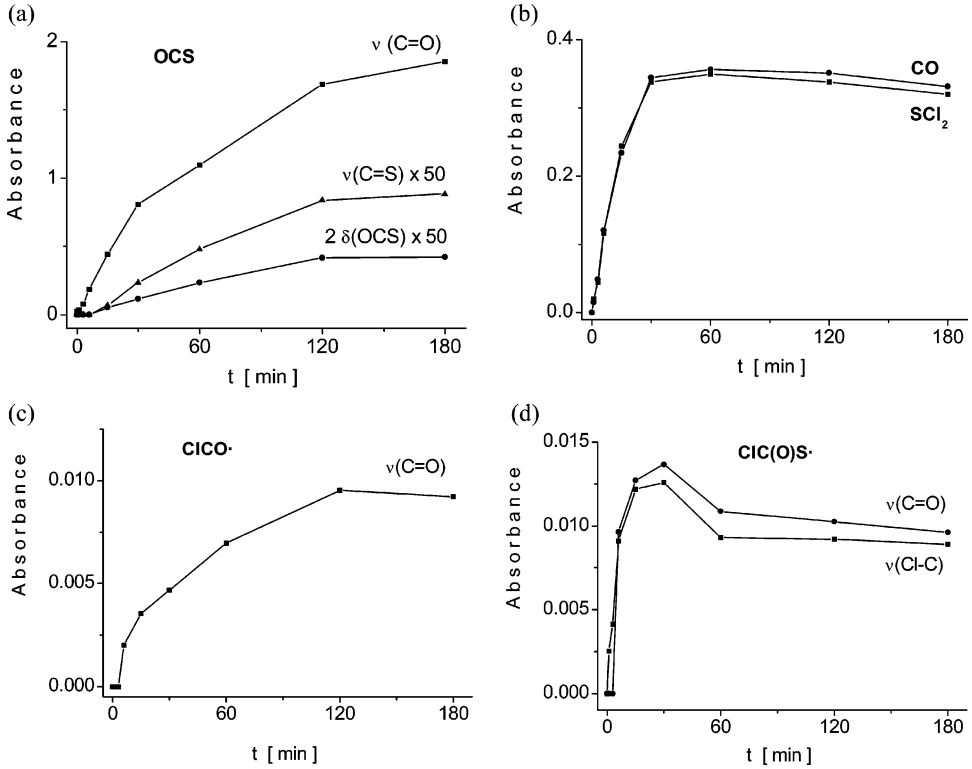

Figure 2. Plots as a function of irradiation time of the intensities of the bands assigned to (a) OCS, (b) CO and SCl_2, (c) ClCO•, and (d) ClCOS• in the IR spectrum of an Ar matrix initially containing ClC(O)SCl.

TABLE 2: Calculated and Experimental IR Wavenumbers and Intensities of the ClC(O)S•· Radical

	HF/6-31+G*		B3LYP/6-31+G*		MP2/6-31+G*		Ar matrix		N_2 matrix	
vibrational mode	ν (cm^{-1})	I_{rel}	ν (cm^{-1})	I_{rel}	ν (cm^{-1})	I_{rel}	ν (cm^{-1})	I_{rel}	ν (cm^{-1})	I_{rel}
ν(C═O)	1811	546	1797	373.4	1762	346.6	1774.8 1773.7[a]	100	1762.6 1760.4[a]	100
ν_{as}(ClCS)	862	404	802	55	873	337	913.5 908.9[a]	87	919.9 918.5 917.8 915.6 914.1[a]	93
δoop(C═O)	629	11	563	<1	569	2				
ν_s(ClCS)	594	47	499	23	551	69				
δ(ClCO)	464	5	403	<1	520	<1				
δ(ClCS)	273	<1	191	<1	242	<1				

[a] Matrix splitting. See text.

ously with photolysis. This is readily identifiable with the formation of OCS.[14] Two other absorptions occurring near 2139 and 520 cm^{-1} grow together during the first hour and then decay somewhat. On the basis of earlier studies, these can be assigned to the molecules CO[15] and SCl_2,[16] respectively. A very weak band near 520 cm^{-1} is also expected from the presence of OCS, attributable to the δ(OCS) fundamental. Considering the relative intensity with respect to the 2050 cm^{-1} fundamental absorption, the behavior as a function of irradiation time, and the characteristic isotopic splitting of this band, we assign it mainly to the SCl_2 molecule. A very weak band appearing near 1876 cm^{-1} may be ascribed to the radical ClCO•, in keeping with the most intense IR feature reported at 1876.7 cm^{-1} when this radical is formed by the addition of Cl atoms to CO molecules and trapped in a solid Ar matrix.[17]

In addition, Figure 2 depicts the behavior of two other IR features that appear on photolysis. Located near 1774 and 913 cm^{-1}, these track each other, growing first and then decaying on continued photolysis, in a way that indicates a common origin. No known product that might be expected to arise from unimolecular photodecomposition of ClC(O)SCl could be recognized as the source of these bands. In these circumstances, we identify the source as the hitherto unknown radical ClCOS•, a conclusion supported by the results of ab initio and DFT calculations. Table 2 lists the wavenumbers calculated for the vibrational fundamentals of this radical by HF, MP2, and B3LYP methods using the 6-31+G* basis sets for comparison with the experimental values. The two fundamentals expected to have the highest intensity in IR absorption are, thus, found to offer a satisfactory explanation of the bands observed near 1774 and 913 cm^{-1}. The dimensions of the radical computed by optimization with simultaneous relaxation of all the geometrical parameters are as follows (MP2/B3LYP; distances in Å, angles in degrees): r(C═O) 1.2060/1.1922, r(C−S) 1.7440/1.7399, r(C−Cl) 1.7742/1.8122, ∠Cl−C−S 110.9/109.8, ∠Cl−C═O 122.9/122.3, and ∠S−C═O 126.2/127.9.

The IR absorptions associated with the OCS, CO, and SCl_2 molecules were typically observed as multiplets. In the case of

TABLE 3: Vibrational Wavenumbers (in cm^{-1}) of *Syn*-ClC(O)SCH_3 and *Syn*-ClC(O)SCD_3

$ClC(O)SCH_3$ Ar matrix	$ClC(O)SCD_3$ Ar matrix	$ClC(O)SCD_3$ N_2 matrix	$ClC(O)SCH_3$ gas[a]	$ClC(O)SCD_3$ gas	assignment
3026.3	2279.5	2273.8	3023	2270	$\nu_{as}(CH_3)$
3019.5	2271.7 2264.1	2268.9 2266.4	3010		$\nu_{as}(CH_3)$
2945.4	2144.7	2145.4 2134.5	2951 2945 2939	2152 2146 2140	$\nu_s(CH_3)$
1769.5	1769.2	1775.9	1788 1777	1786 1775	$\nu(C{=}O)$
1677.2	1678.8	1691.7		1694	$\rho(CH_3) + \nu(S{-}CH_3)$
1433.6 1420.0	1044.8 1035.6}	1045.7 1045.0 1037.2	1444 1433 1421	1049 1039	$\delta_{as}(CH_3)$
1320.4	990.2 984.7	998.7 993.1	1330 1322	1001 995	$\delta_s(CH_3)$
972.1 964.9	671.8 663.5	678.3	977 970	668	$\rho(CH_3)$
859.7 856.7 849.9	862.6 857.1 848.4 842.3	868.2 865.6 862.9 855.7 854.1	872 863	874 870 863	$\nu_{as}(S{-}C{-}Cl)$
711.7	661.9	662.3	725		$\nu(S{-}CH_3)$
580.2 578.5	563.7 561.7	569.1 567.2	585 578	572 564	$\nu_s(S{-}C{-}Cl)$
574.3	573.7	575.2 574.5			$\delta(Cl{-}C{-}O)$
431.2 427.6	426.5 422.6	429.7 429.1	439	~435	$\rho(C{=}O)$

[a] Nyquist, R. A. *J. Mol. Struct.* **1967**−**1968**, *1*, 1.

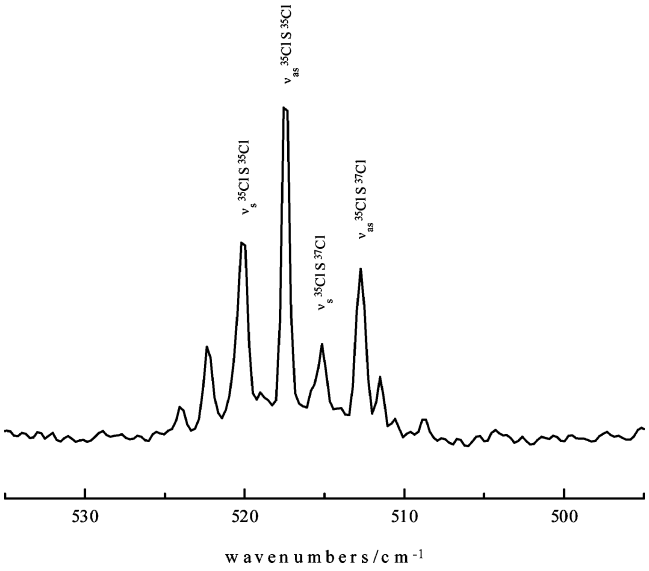

Figure 3. IR spectrum of the SCl_2 molecule formed in an Ar matrix containing ClC(O)SCl after 180 min of broad-band UV−visible photolysis.

SCl_2, the intensity pattern of the multiplet centered near 520 cm^{-1} remained constant during photolysis and can be identified with overlapping of the symmetric and antisymmetric ν(S−Cl) modes for the different isotopomers $S^{35}Cl_2$, $^{35}ClS^{37}Cl$, and $S^{37}Cl_2$ (see Table 1 and Figure 3). However, the other two species, OCS and CO, were observed to display rather more complicated behavior, with different components of the multiplet patterns appearing at different irradiation times. This we attribute to the perturbing influence of other photoproducts constrained by the rigidity of the matrix host either to occupy the same matrix cage as the CO or OCS or to form part of that cage. Such behavior has been noted previously for CO.[15] Although some van der Waals complexes of halogen, interhalogen, and other molecules with CO[18] and OCS[19,20] have also been characterized recently, the variety of photoproducts yielded by ClC(O)SCl rules out any identification of the individual perturbing molecules in this case.

Photolysis of Normal and Perdeuterated ClC(O)SCH_3. The IR spectra of $ClC(O)SCH_3$ isolated in Ar and N_2 matrixes have been described previously.[10] We have now also measured the IR spectra of $ClC(O)SCD_3$ in the vapor phase and isolated in Ar and N_2 matrixes. The relevant wavenumbers are given in Table 3, together with the corresponding data for $ClC(O)SCH_3$; the proposed assignments are supported by the results of quantum chemical calculations.[10]

Exposure of an Ar or N_2 matrix doped with ~0.1% $ClC(O)SCH_3$ or $ClC(O)SCD_3$ to broad-band UV−visible light resulted in the appearance and growth of several new bands, as listed in Table 4. Figure 4 shows the IR spectra of the syn conformer of $ClC(O)SCH_3$ isolated in an Ar matrix before and after irradiation, whereas Figure 5 depicts the integrated intensities of some of the bands as a function of irradiation time. The IR bands originating in *syn*-$ClC(O)SCH_3$, shown in Figure 5a, are thus seen to decay on irradiation. A group of new absorptions near 2140 cm^{-1} grew continuously on photolysis, the intensities tending asymptotically to limiting values in a way that complements the decay of the original *syn*-$ClC(O)SCH_3$. This is identifiable[15] with the formation of CO (Figure 5b). As with the features assigned to CO in the photolysis of ClC(O)SCl,

TABLE 4: Vibrational Wavenumbers (in cm^{-1}) and Assignments of the IR Absorptions Appearing after Broad-Band UV−Visible Photolysis of $ClC(O)SCH_3$ and $ClC(O)SCD_3$ Isolated in an Ar or N_2 Matrix

$ClC(O)SCH_3$		$ClC(O)SCD_3$		assignment		wavenumber
Ar matrix	N_2 matrix	Ar matrix	N_2 matrix	molecule	vibrational mode	reported previously
3013.6	3012.0	2262.6	2263.2	$ClSCH_3$	$\nu_{as}CH_3$	3009[a]
2999.8 2993.5	3001.4	2250.2 2245.1 2242.8	2250.2	$ClSCH_3$	$\nu_{as}CH_3$	2993[a]
2971.6 2962.6	2977.6		2235.4	$H_2CS\cdots HCl$	νC−H	
2932.9 2928.7	2931.2	2135.1	2135.2	$ClSCH_3$	ν_sCH_3	2927[a]
2505.3 2477.6 2456.7	2513.0 2500.9 2456.6	1830.4 1812.4 1797.6	1836.9 1828.3	$H_2CS\cdots HCl$	νH−Cl	
2146.1 2144.1 2142.1 2140.2 2138.6 2137.1 2135.1	2145.4 2144.0 2142.8 2141.1 2139.2	2146.2 2144.3 2142.2 2140.1 2137.0 2135.1	2143.9 2142.8 2141.1 2139.3	CO	νC═O	2138.2[b]
1439.2	1440.6 1439.2	1053.1	1053.3 1052.0	$ClSCH_3$	$\delta_{as}CH_3$	1436[a]
1413.5 1406.8	1412.1	1028.9 1025.7	1029.1	$ClSCH_3$	$\delta_{as}CH_3$	1406[a]
1315.9 1314.6 1312.3	1320.2 1319.0 1317.6	1017.0	1018.5	$ClSCH_3$	δ_sCH_3	1315[a]
1051.6 1050.6	1059.4 1056.0	932.6 931.6	936.6	$H_2CS\cdots HCl$	νS═C	
999.6	1002.5 1000.9 999.4	789.0	789.1 787.8	$H_2CS\cdots HCl$	ρCH_2	
992.7 991.7	995.5	784.0		$H_2CS\cdots HCl$		
966.4 963.8	974.6	765.1 758.4	771.0 763.9	$ClSCH_3$	ρCH_3	964[a]
957.8 954.5	964.1	732.1 730.5		$ClSCH_3$	ρCH_3	957[a]
706.0	713.4	652.4	659.7	$ClSCH_3$	νC−S	705[a]
517.5 516.1	523.4 521.6	511.7 510.4	518.0 516.3 514.8 513.1	$ClSCH_3$	νS−^{35}Cl	523[a]
510.9 509.7	517.9 516.8	505.1 503.8	511.3 509.6 507.9 506.5	$ClSCH_3$	νS−^{37}Cl	517[a]

[a] Ref 21. [b] Ref 18.

the rather complicated multiplet pattern must reflect the different interactions between the CO molecule and other photofragments.

Figure 5c traces the intensities of four bands centered near 1439, 954, 706, and 516 cm^{-1} which exhibit a common pattern in their initial growth and subsequent decay on continued photolysis. These new absorptions clearly arise from the molecule CH_3SCl, the wavenumbers being close to those of the most intense features in the IR spectrum reported[21] for the pure compound isolated in solid Ar. Further support for this identification comes from two sources: (i) the observation of all the fundamentals reported previously[21] for the molecules CH_3SCl and CD_3SCl (see Table 4) and (ii) the characteristic splitting of ~6 cm^{-1} of the ν(S−Cl) fundamental near 515 cm^{-1} due to the naturally occurring isotopic pair $^{35}Cl/^{37}Cl$.

As the intensities of the IR absorptions arising from the intermediate photoproduct CH_3SCl (or CD_3SCl) decreased, other absorptions were observed to develop with intensities reaching constant limiting values at the end of the experiment. The behavior suggests that the new features are carried by the photodecomposition product or products of the sulfenyl chloride (Figure 5d). Taking into account the wavenumber shifts observed on photolysis of the deuterated compound, we conclude that some of the absorptions—those appearing near 1051 and 999 cm^{-1} (Figure 5d), together with the less intense features near 2962 and 992 cm^{-1} (see Table 4)—are identifiable with the formation of thioformaldehyde, $S{=}CH_2$.[22] The remaining band, near 2505 cm^{-1} and the most intense feature in Figure 5d, must then be due to HCl in a loosely bound complex with

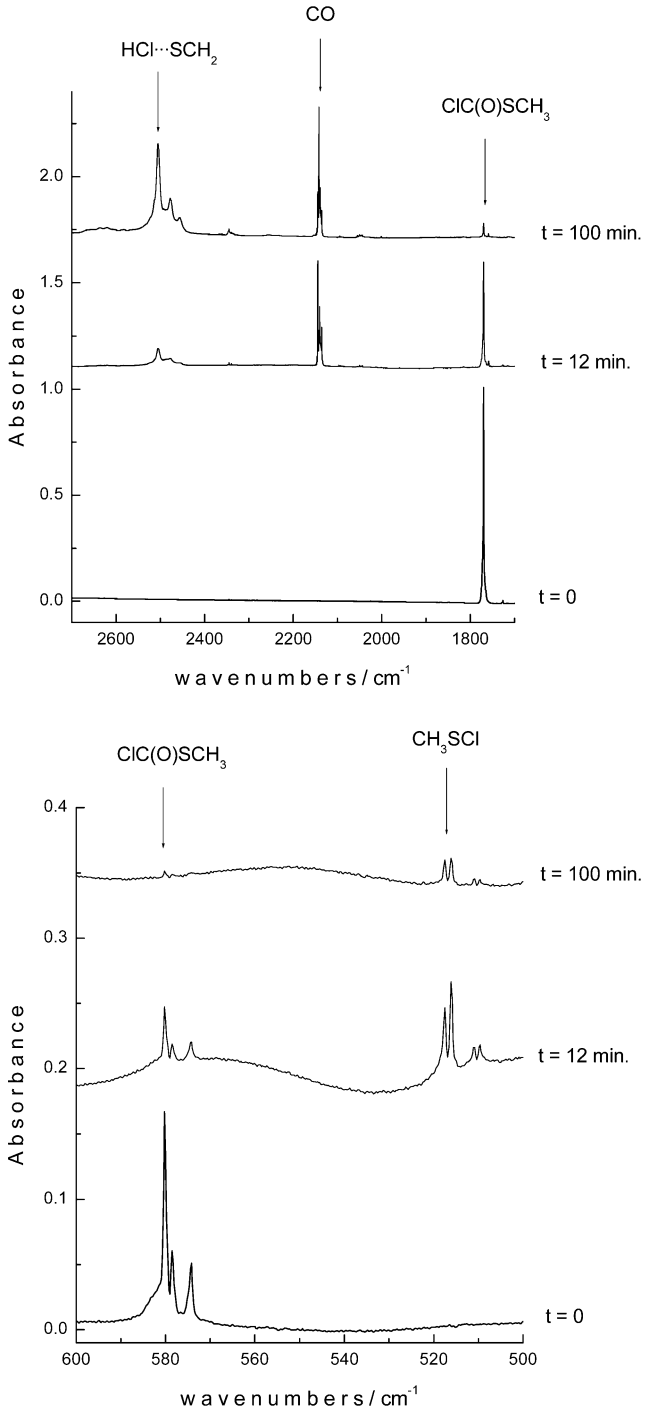

Figure 4. IR spectra of an Ar matrix containing $ClC(O)SCH_3$ at different irradiation times in the regions 1700−2700 cm^{-1} (top) and 500−600 cm^{-1} (bottom).

S═CH_2. Free monomeric HCl isolated in solid Ar absorbs at 2871 cm^{-1} [23] so that complexation results in a red shift of ∼364 cm^{-1} for the ν(H−Cl) fundamental. This is comparable with the perturbation observed in alcohol complexes R(H)O·HCl ($\Delta\nu$ = −359 and −370 cm^{-1} for R = Me and Et, respectively) but rather less than for Me_2S·HCl ($\Delta\nu = -604$ cm^{-1}) under similar conditions.[24] Hence, the hydrogen bonding in H_2C═S·HCl is relatively strong. Further evidence in support of such a complex comes from the shift of the 2505 cm^{-1} absorption to ∼1830 cm^{-1} (H/D = 1.369:1) when $ClC(O)SCD_3$ is the precursor and from the theoretical calculations described below.

Theoretical Study of the H_2C═S···HCl Molecular Complex. Equilibrium Geometry. Simple molecular orbital pictures of thioformaldehyde imply two possible structures for H_2C═S···HCl. If HCl interacts with the highest occupied π-type molecular orbital, the structure is expected to be T-shaped with the HCl axis perpendicular to the H_2C═S plane and roughly bisecting the C═S axis. The other possibility is an interaction with the n-type molecular orbitals associated with the S atom, suggesting a bent, planar structure for the complex. According to simple models, then, the C═S···H angle should be close to 90° in either case.

SCHEME 2: Possible Forms of the H_2C═S···HCl Molecular Complex.

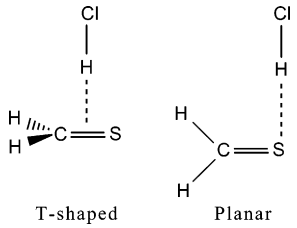

Attempts to optimize a T-shaped structure with no imaginary frequencies failed for both MP2 and B3LYP approximations. For the planar structure, a potential energy scan as a function of the S···H intermolecular distance was performed using the B3LYP/6-31+G* theoretical model. Figure 6 shows the resulting potential energy curve when the S···H intermolecular distance is varied from 2.0 to 5.0 Å in steps of 0.1 Å. The structure corresponding to the energy minimum occurring at an intermolecular distance of 2.3 Å was subsequently used as a starting geometry for a full structure optimization. Table 5 lists the dimensions of the stable form calculated with different theoretical models, together with the corresponding dimensions of the free subunits at the same level of approximation. Figure 7 shows a molecular model of the complex as calculated with the B3LYP/6-31+G* approximation.

Binding Energy. The binding energy was calculated using the correction proposed by Nagy et al.[25] and expressed by eq 1,

$$\Delta E^{c} = \Delta E - \mathrm{BSSE} + \mathrm{GEOM} \quad (1)$$

where ΔE^{c} and ΔE are the corrected and uncorrected binding energies, respectively, BSSE corresponds to the error due to the basis set superposition, and the term GEOM takes into account the geometry differences between free S═CH_2 and HCl monomers and each of the subunits as they occur in the complex. These terms can be calculated through eqs 2−4,

$$\Delta E = E(\mathrm{AB}) - E^{\mathrm{m,m}}(\mathrm{A}) - E^{\mathrm{m,m}}(\mathrm{B}) \quad (2)$$

$$\mathrm{BSSE}_{(\mathrm{d,d-d,m})} = E^{\mathrm{d,d}}(\mathrm{A}) - E^{\mathrm{d,m}}(\mathrm{A}) + E^{\mathrm{d,d}}(\mathrm{B}) - E^{\mathrm{d,m}}(\mathrm{B}) \quad (3)$$

$$\mathrm{GEOM}_{(\mathrm{d,m-m,m})} = E^{\mathrm{d,m}}(\mathrm{A}) - E^{\mathrm{m,m}}(\mathrm{A}) + E^{\mathrm{d,m}}(\mathrm{B}) - E^{\mathrm{m,m}}(\mathrm{B}) \quad (4)$$

where the superscripts m and d refer to the monomers and dimer (complex), respectively. The first superscript refers to the geometry of the species, and the second one refers to the basis set used to calculate the energy at a geometry defined by the first superscript. The BSSE terms have been calculated by applying the counterpoise procedure developed by Boys and Bernardi.[26]

Values of +4.19 and +4.13 kcal mol^{-1} were calculated with the B3LYP/6-31+G* theoretical model for the uncorrected (ΔE) and corrected (ΔE^{c}) binding energies, respectively, the small

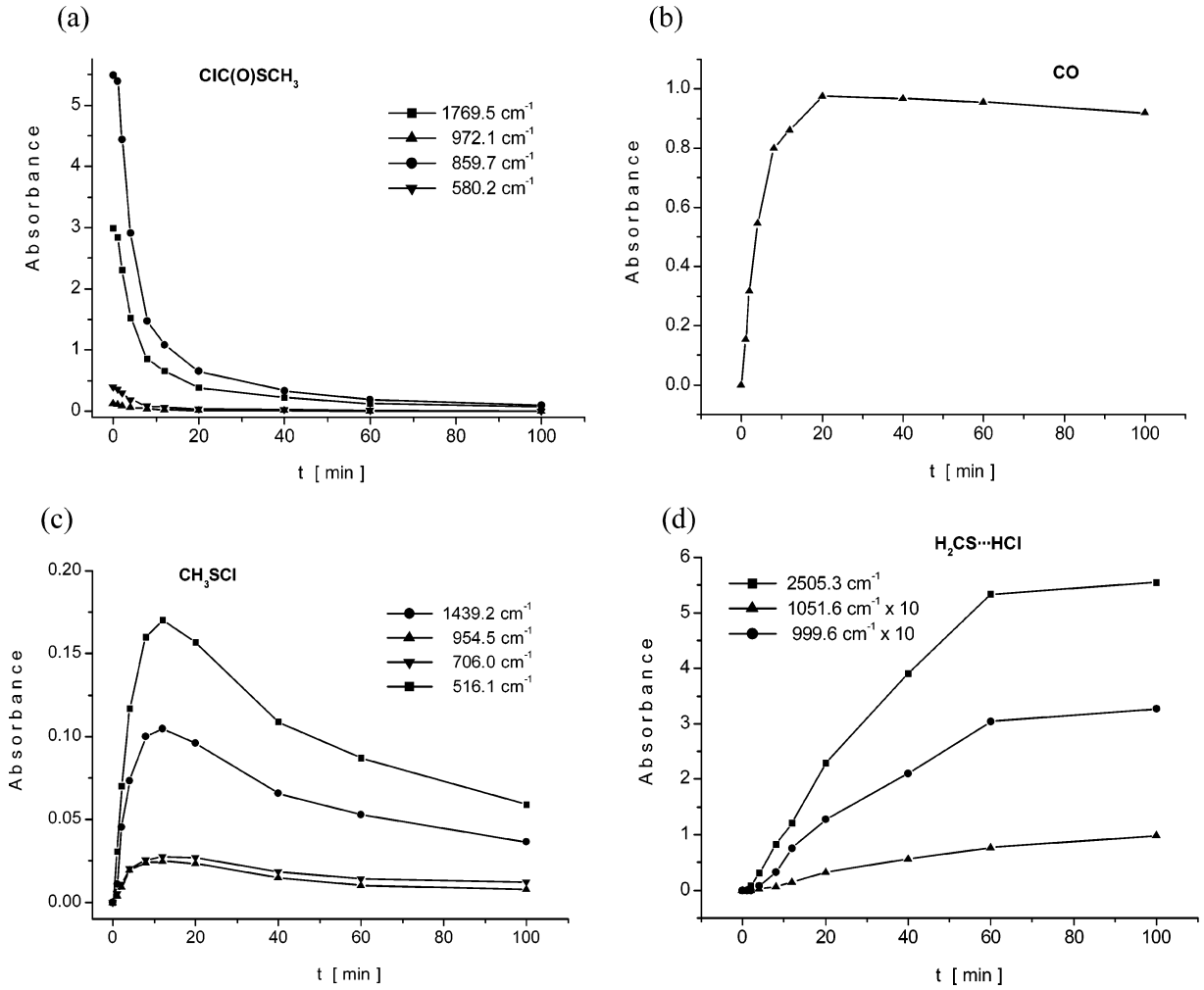

Figure 5. Plots as a function of irradiation time of the intensities of the bands assigned to (a) $ClC(O)SCH_3$, (b) CO, (c) $ClSCH_3$, and (d) $H_2CS\cdots HCl$ in the IR spectrum of an Ar matrix initially containing $ClC(O)SCH_3$.

TABLE 5: Geometric Parameters of the $H_2C{=}S\cdots HCl$ Molecular Complex and of the HCl and $H_2C{=}S$ Monomers Calculated with Different Theoretical Models (Distances in Å, Angles in Degrees)

geometric parameter	B3LYP/6-31+G*				MP2/6-31+G*			
	$H_2C{=}S\cdots HCl$	HCl_{free}	$H_2C{=}S_{free}$	ΔGP [a]	$H_2C{=}S\cdots HCl$	HCl_{free}	$H_2C{=}S_{free}$	ΔGP [a]
r[S···H(1)]	2.3393				2.4606			
r[H(1)−Cl]	1.3159	1.2904		+0.0255	1.2934	1.2810		+0.0124
r[C=S]	1.6214		1.6200	+0.0014	1.6198		1.6186	+0.0012
r[C−H(2)]	1.0922		1.0930	−0.0008	1.0907		1.0903	+0.0004
r[C−H(3)]	1.0915		1.0930	−0.0015	1.0897		1.0904	−0.0007
α[S···H(1)−Cl]	167.1				163.1			
α[C=S···H(1)]	92.6				88.5			
α[H(2)−C=S]	122.3		122.3	0.0	122.1		121.9	+0.2
α[H(3)−C=S]	121.7		122.3	−0.6	121.5		121.9	−0.4
α[H(2)−C-H(3)]	116.0		115.4	+0.6	116.4		116.2	+0.2
τ[H(2)C=S···H(1)]	0.0				0.0			
τ[C=S···H(1)−Cl]	0.0				0.0			

[a] Difference between the geometric parameters in the complex and in the free molecule.

difference between these two quantities being mainly attributable to the near-cancellation of the terms BSSE (−0.29 kcal mol^{-1}) and GEOM (+0.23 kcal mol^{-1}) in eq 1.

Vibrational Properties. Details of the IR spectra computed (B3LYP/6-31+G* and MP2/6-31+G*) for the complex are presented in Table 6, together with the corresponding properties of the two free subunits estimated at the same level of approximations and the experimental wavenumbers for both the complex and free monomers isolated in Ar matrixes. Where comparisons can be made, there is good agreement between the theoretical and experimental wavenumber shifts induced by complexation of the free subunits, particularly in the case of the ν(H−Cl) vibrational mode for which a predicted shift of −371 cm^{-1} (B3LYP/6-31+G*) is matched experimentally by a shift of −364 cm^{-1}. Small shifts for the fundamentals of the other subunit in the complex, that is, $H_2C{=}S$, are predicted by the theoretical calculations, and these, too, generally reproduce well the experimental values.

NBO Analysis. Natural bond orbital (NBO) analysis was performed to investigate the bonding properties of the complex $H_2C{=}S.HCl$ as interpreted in terms of "donor−acceptor" interactions.[27] According to this analysis, the amount of charge

TABLE 6: Calculated and Experimental Vibrational Wavenumbers (in cm^{-1}) of the $H_2C{=}S{\cdots}HCl$ Molecular Complex and of the Free HCl and $H_2C{=}S$ Monomers

B3LYP/6-31+G*				MP2/6-31+G*				Ar matrix				
$H_2C{=}S{\cdots}HCl$	HCl	$H_2C{=}S$	$\Delta\nu$	$H_2C{=}S{\cdots}HCl$	HCl[a]	$H_2C{=}S$[b]	$\Delta\nu$	$H_2C{=}S{\cdots}HCl$	HCl	$H_2C{=}S$	$\Delta\nu$	assignment
3194.8		3169.5	+25.3	3254.6		3244.2				3024.6		$\nu_{as}CH_2$
3105.5		3088.7	+16.8	3155.9		3150.3	+5.6	2962.6		2971.0	−8.4	ν_sCH_2
2550.1	2921.4		−371.3	2846.5	3035.9		−189.4	2505.3	2871		−364	νH−Cl
1519.1		1521.7	−2.6	1558.0		1556.0	+2.0			1457.3		δCH_2
1076.7		1081.0	−4.3	1106.6		1106.7	−0.1	1051.6		1059.2	−7.6	νC=S
1039.3		1031.1	+8.2	1059.5		1054.7	+4.8	999.6		991.0	+8.6	δCH_2 oop.
1019.6		1020.5	−0.9	1053.5		1043.8	+9.7	992.7		990.2	+2.5	ρCH_2
501.8				434.0								δCl−H···S
459.1				385.7								δCl−H···S oop
214.5				186.4								t
119.9				116.1								νS···H
49.5				59.2								dC=S···H

[a] Ref 23. [b] Ref 22.

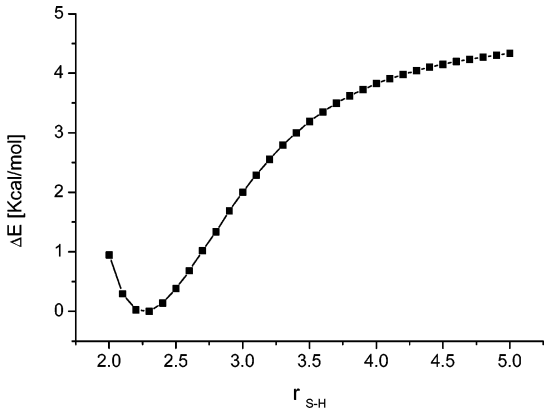

Figure 6. Potential energy curve as a function of the S···H intermolecular distance for the planar form of the $H_2CS{\cdots}HCl$ complex calculated with the B3LYP/6-31+G* theoretical model.

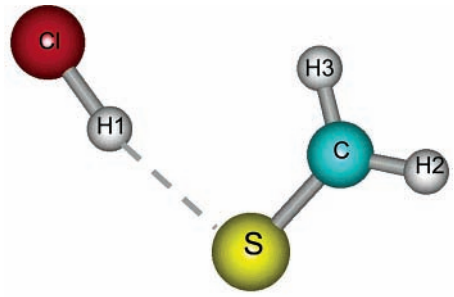

Figure 7. Molecular model of the $H_2CS{\cdots}HCl$ complex optimized with the B3LYP/6-31+G* theoretical model.

transferred (q) from the $H_2C{=}S$ subunit to the HCl subunit totals 0.0775e. The largest contribution to the stabilization energy arises from the interaction of the lone pair of the S atom of $H_2C{=}S$ with the unfilled σ antibonding orbital of the HCl molecule. This energy lowering could be expressed by the following second-order equation

$$\Delta E_{n\sigma^*}(H_2C{=}S{\cdots}HCl) = -2\frac{\langle n_S|\hat{F}|\sigma^*_{HCl}\rangle^2}{\epsilon_{\sigma_{HCl}{}^*} - \epsilon_{nS}} \qquad (5)$$

in which F is the Fock operator and ϵ's are the orbital energies. The calculated value for the energy lowering due to this interaction, according to the B3LYP/6-31+G* calculations, is 16.76 kcal mol^{-1}.

SCHEME 3: Outline of Reactions Occurring on Broad-Band UV−Visible Photolysis of Matrix-Isolated ClC(O)SCl.

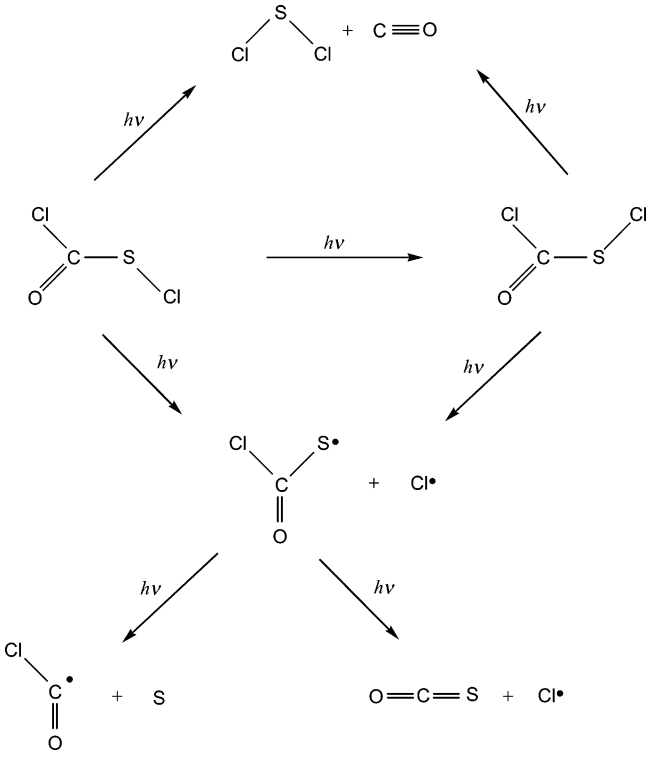

Conclusions

The matrix photochemistries of each of the (chlorocarbonyl)-sulfenyl compounds ClC(O)SCl and $ClC(O)SCH_3$ are characterized by two distinct, primary pathways [in addition to conformational change in the case of ClC(O)SCl], as depicted in Schemes 3 and 4. The reaction channels have been identified as a result of the characterization of the various photoproducts by their IR spectra and of the observed behaviors of the IR absorptions as a function of irradiation time.

The photolytic interconversion of the two rotamers of ClC(O)SCl is the first process observed on broad-band UV−visible irradiation of the matrix-isolated ClC(O)SCl molecule, behavior made familiar by analogous studies of other sulfenyl carbonyl compounds, for example, ClC(O)SBr,[5] FC(O)SCl,[1] and FC(O)SBr.[2] Both forms of ClC(O)SCl then suffer photodecomposition by two distinct reaction channels. One of these leads to CO and SCl_2 molecules as photostable products and, thus,

SCHEME 4: Outline of Reactions Occurring on Broad-Band UV−Visible Photolysis of Matrix-Isolated $ClC(O)SCH_3$.

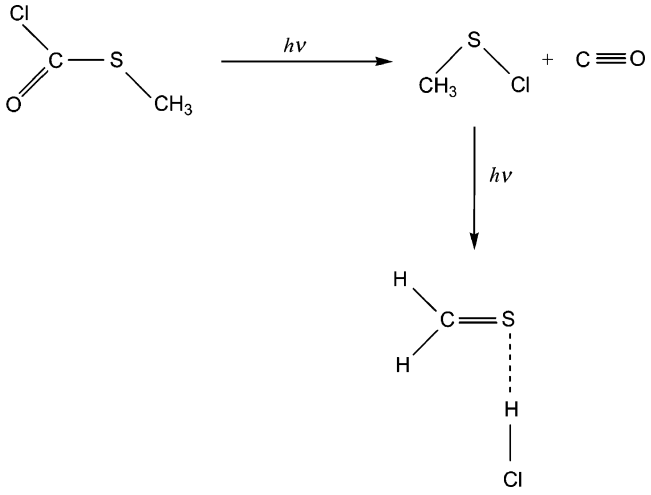

parallels similar photochemical changes in which CO is extruded, for example, from $ClC(O)SBr$,[5] $FC(O)SCl$,[28] and $FC(O)SBr$.[2] A competing decomposition channel gives rise to the formation of the hitherto unknown $ClC(O)S^{\bullet}$ radical and presumably also to $Cl^{\bullet}$ atoms. This radical is not photostable under the conditions of our experiments and subsequently decomposes, also via two different channels. The first gives rise to the $ClCO^{\bullet}$ radical (plus a sulfur atom), and the other, to the OCS molecule (plus a chlorine atom).

On the other hand, replacement of the Cl bound to sulfur by CH_3 in $ClC(O)SCH_3$ results in quite different matrix photochemistry in which two main channels are again discernible, but now in sequence rather than in parallel. In the first place, the compound decomposes to give CO and $ClSCH_3$ molecules. In the second step, a hydrogen atom is detached from the methyl group of $ClSCH_3$, and HCl is eliminated through the formation of a molecular complex between HCl and $H_2C{=}S$ (Scheme 4).

Acknowledgment. The authors acknowledge with thanks a British Council−Fundación Antorchas award for British−Argentine cooperation. C.O.D.V. and R.M.R. thank the Jesus College of Oxford, Consejo Nacional de Investigaciones Científicas y Técnicas (CONICET) (PIP 4695), Comisión de Investigaciones Científicas de la Provincia de Buenos Aires (CIC), and Facultad de Ciencias Exactas, Universidad Nacional de La Plata for financial support. R.M.R. also acknowledges with gratitude Fundación Antorchas and a Royal Society of Chemistry grant for international authors. In addition, A.J.D. is indebted to the EPSRC for support, including the purchase of equipment.

References and Notes

(1) Mack, H.-G.; Oberhammer, H.; Della Védova, C. O. *J. Phys. Chem.*, **1991**, *95*, 4238.

(2) Della Védova, C. O.; Mack, H.-G. *Inorg. Chem.* **1993**, *32*, 948.

(3) Mack, H.-G.; Oberhammer, H.; Della Védova, C. O. *J. Mol. Struct*. **1992**, *265*, 347.

(4) Mack, H.-G.; Della Védova, C. O.; Oberhammer, H. *J. Phys. Chem.* **1992**, *96*, 9215.

(5) Romano, R. M.; Della Védova, C. O.; Downs, A. J.; Greene, T. M. *J. Am. Chem. Soc.* **2001**, *123*, 5794.

(6) Romano, R. M.; Della Védova, C. O.; Downs, A. J. *J. Phys. Chem. A* **2002**, *106*, 7235.

(7) Romano, R. M.; Della Védova, C. O.; Downs, A. J. Unpublished results.

(8) Romano, R. M.; Della Védova, C. O.; Downs, A. J. Unpublished results.

(9) Romano, R. M.; Della Védova, C. O.; Downs, A. J. *Chem. Commun.* **2001**, 2638.

(10) Romano, R. M.; Della Védova, C. O.; Downs, A. J.; Parsons, S.; Smith, C. *New J. Chem.* **2003**, *27*, 514.

(11) Almond, M. J.; Downs, A. J. *Adv. Spectrosc.* **1989**, *17*, 1. Dunkin, I. R. *Matrix-Isolation Techniques: A Practical Approach*; Oxford University Press: New York, 1998.

(12) Perutz, R. N.; Turner J. J. *J. Chem. Soc., Faraday Trans. 2* **1973**, *69*, 452.

(13) Frisch, M. J.; Trucks, G. W.; Schlegel, H. B.; Scuseria, G. E.; Robb, M. A.; Cheeseman, J. R.; Zakrzewski, V. G.; Montgomery, J. A., Jr.; Stratmann, R. E.; Burant, J. C.; Dapprich, S.; Millam, J. M.; Daniels, A. D.; Kudin, K. N.; Strain, M. C.; Farkas, O.; Tomasi, J.; Barone, V.; Cossi, M.; Cammi, R.; Mennucci, B.; Pomelli, C.; Adamo, C.; Clifford, S.; Ochterski, J.; Petersson, G. A.; Ayala, P. Y.; Cui, Q.; Morokuma, K.; Malick, D. K.; Rabuck, A. D.; Raghavachari, K.; Foresman, J. B.; Cioslowski, J.; Ortiz, J. V.; Baboul, A. G.; Stefanov, B. B.; Liu, G.; Liashenko, A.; Piskorz, P.; Komaromi, I.; Gomperts, R.; Martin, R. L.; Fox, D. J.; Keith, T.; Al-Laham, M. A.; Peng, C. Y.; Nanayakkara, A.; Gonzalez, C.; Challacombe, M.; Gill, P. M. W.; Johnson, B.; Chen, W.; Wong, M. W.; Andres, J. L.; Head-Gordon, M.; Replogle, E. S.; Pople, J. A. *Gaussian 98*, Revision A.7; Gaussian, Inc.: Pittsburgh, PA, 1998.

(14) Verderame, F. D.; Nixon, E. R. *J. Chem. Phys*. **1966**, *44*, 43. Hawkins, M.; Almond, M. J.; Downs, A. J. *J. Phys. Chem*. **1985**, *89*, 3326. Lang, V. I.; Winn, J. S. *J. Chem. Phys*. **1991**, *94*, 5270.

(15) Dubost, H. *Chem. Phys*. **1976**, *12*, 139.

(16) Bielefeldt, D.; Willner, H. *Spectrochim. Acta, Part A* **1980**, *36*, 989.

(17) Schnöckel, H.; Eberlein, R. A.; Plitt, H. S. *J. Chem. Phys*. **1992**, *97*, 4.

(18) Romano, R. M.; Downs, A. J. *J. Phys. Chem. A* **2003**, *107*, 5298.

(19) Andrews, L.; Bohn, R. B.; Arlinghaus, R. T.; Hunt, R. D. *Chem. Phys. Lett*. **1989**, *158*, 564. van der Veken, B. J.; Sluyts, E. J.; Herrebout, W. A. *J. Mol. Struct*. **1998**, *449*, 219.

(20) Romano, R. M.; Della Védova, C. O.; Downs, A. J. Unpublished results.

(21) Saito, H.; Kurabe, H.; Suzuki, E.; Watari, F. *Spectrochim. Acta, Part A* **1995**, *51*, 2447.

(22) Clouthier, D. J.; Ramsay, D. A. *Annu. Rev. Phys. Chem*. **1983**, *34*, 31.

(23) Maillard, D.; Schriver, A.; Perchard, J. P.; Girardet, C.; Robert, D. *J. Chem. Phys*. **1977**, *67*, 3917.

(24) Barnes, A. J. *J. Mol. Struct*. **1983**, *100*, 259.

(25) Nagy, P. I.; Smith, D. A.; Alagona, G.; Ghio, C. *J. Phys. Chem*. **1994**, *98*, 486.

(26) Boys, S. F.; Bernardi, F. *Mol. Phys*. **1970**, *19*, 553.

(27) Reed, A. E.; Curtiss, L. A.; Weinhold, F. *Chem. Rev*. **1988**, *88*, 899.

(28) Willner, H. *Z. Naturforsch. B: Anorg. Chem., Org. Chem.* **1984**, *39*, 314.